Eur. J. Mineral.
2008, **20**, 721–734
Published online October 2008

This paper is dedicated to the memory of Werner Schreyer

Sapphirine-bearing assemblages in the system $MgO–Al_2O_3–SiO_2$: a continuing ambiguity

KONSTANTIN K. PODLESSKII[1,*], LEONID Y. ARANOVICH[1,2], TARAS V. GERYA[3] and NATALIA A. KOSYAKOVA[1]

[1]Institute of Experimental Mineralogy, Russian Academy of Sciences, 142432 Chernogolovka, Moscow, Russia
*Corresponding author, e-mail: kkp@iem.ac.ru
[2]Institute of Geology of Ore Deposits, Petrography, Mineralogy and Geochemistry (IGEM), Russian Academy of Sciences, Staromonetny per. 35, 119017 Moscow, Russia
[3]Institute of Geophysics, Department of Geosciences, Swiss Federal Institute of Technology (ETH – Zürich), ETH – Hönggerberg, HPP, 8093 Zürich, Switzerland

Abstract: Based on experimental data for reactions involving sapphirine in the system $MgO–Al_2O_3–SiO_2$ (MAS), thermodynamic properties of the sapphirine solid solution end-members have been optimized for both ideal and non-ideal models, and internally consistent P–T grids are proposed. According to the calculated P–T relationships in MAS, the sapphirine + quartz assemblage, which is widely recognized as indicative of ultrahigh-temperature metamorphism, can be stable down to 840 °C and 0.67 GPa, *i.e.*, at temperatures up to 150 °C lower than estimated by Kelsey *et al*. (2004). The sapphirine + kyanite assemblage has been found stable at temperatures below 860 °C and 1.13 GPa, whereas the sapphirine + forsterite assemblage may be stable below 800 °C only under specific conditions of a very low activity of water. Calculations of P–T relationships involving sapphirine using the THERMOCALC dataset revealed its inconsistency with both experimental and natural assemblages.

Key-words: sapphirine, $MgO–Al_2O_3–SiO_2$, thermodynamic data, ultrahigh-temperature metamorphism.

Introduction

This work is dedicated to the memory of Werner Schreyer, who came to an understanding about the importance of sapphirine for estimating metamorphic conditions long ago while working on the phase relationships of cordierite in the beginning of 1960s (Schreyer & Yoder, 1960; Schreyer & Schairer, 1961a and b). Schreyer later made significant contributions that illuminated different aspects of sapphirine behavior both in experimental systems and in natural rocks (Schreyer, 1967, 1968; Schreyer & Seifert, 1969a and b, 1970; Schreyer & Abraham, 1975; Schreyer *et al*., 1975, 1984, as well as other publications with co-workers cited below).

Assemblages of sapphirine, once considered to be a rare mineral, have in recent years been recognized as important indicators of relatively high-temperature metamorphism. Sapphirine occurs in rocks that have undergone different tectono-metamorphic histories, with the P–T range of formation being estimated from below 700 °C and 0.5 GPa to above 1100 °C and 1.5 GPa. Sapphirine associated with quartz is attributed exclusively to the highest temperature conditions of crustal metamorphism referred to as "ultrahigh-temperature metamorphism" (Harley, 1998).

Although experimental data involving sapphirine extend over an even wider P–T range, the quantitative interpretation of sapphirine-bearing assemblages remains ambiguous, and thermodynamic properties of sapphirine are still poorly understood. In part, this is because experimental reversals of equilibria involving sapphirine have been obtained only in the model system $MgO–Al_2O_3–SiO_2$ (MAS), and only Hollis & Harley (2003) have attempted to measure the compositions of sapphirine solid solution in such experiments. Because the experimental data were insufficient to substantiate an unambiguous thermodynamic description of the MAS system, Gasparik (1994) and Podlesskii (1995) independently deduced petrogenetic grids differing from one another both quantitatively and qualitatively. Internally consistent thermodynamic datasets (Gerya *et al*., 1996; Holland & Powell, 1998), with their later modifications (Ouzegane *et al*., 2003; Gerya *et al*., 2004a; Kelsey *et al*., 2004), also imply significantly different phase relationships for key sapphirine-bearing assemblages even in this simple system.

In this contribution, we consider only MAS assemblages, because experimental studies of more complex systems, beginning with the pioneering work by Hensen & Green (1971), are restricted to synthesis or crystallization experiments, with no bracketing by reversal, which do not provide a firm foundation for thermodynamic modeling (Berman & Aranovich, 1996). It is noteworthy that those who carried out experiments involving sapphirine in more complex systems such as $FeO–MgO–Al_2O_3–SiO_2$ (FMAS), $K_2O–FeO–MgO–Al_2O_3–SiO_2$ and $K_2O–Na_2O–FeO–MgO–Al_2O_3–SiO_2$, did not attempt to use their own data to extract

DOI: 10.1127/0935-1221/2008/0020-1870
0935-1221/08/0020-1870 $ 6.30

thermodynamic characteristics of sapphirine end-members or mixing properties, but restricted application to qualitative graphical analysis of phase relations (Hensen, 1986; Hensen & Harley, 1990), although these were plotted on quantitative P–T diagrams (Harley, 1998, 2008; Das *et al*., 2001, 2003). Calibrations of Fe–Mg exchange reactions between sapphirine and other minerals based on experimental crystallization of complex mixtures did not provide evidence for achieving equilibrium relationships, and conflicting results were obtained in experiments using the same approach (Das *et al*., 2006; Sato *et al*., 2006).

Other components that enter sapphirine, *i.e*., Fe^{3+}, Be (Christy *et al*., 2002; Christy & Grew, 2004; Grew *et al*., 2006 and the references therein), B (Grew *et al*., 1990, 1992), Ca (Grew *et al*., 1992), Cr (Friend, 1982; Brigida *et al*., 2007) and Ti (Harley & Christy, 1995; Sheng *et al*., 1991) undoubtedly play important roles in expanding the stability of sapphirine relative to the model system MAS, but these components are also beyond consideration in this paper.

Here we present new models of the thermodynamic properties of magnesian sapphirine. Phase relations involving sapphirine in MAS derived with these data are tested with existing experimental constraints. Our parameters differ from the data used in THERMOCALC (Kelsey *et al.*, 2004) and seem to describe the experimentally studied reactions better. For the estimated stability of assemblages of sapphirine with quartz, kyanite and forsterite, to which we have paid special attention due to their petrologic importance, these differences are dramatic, and may change the interpretations of petrogenetic processes.

Sapphirine solid solution and its thermodynamic model in MAS

After the structure determination by Moore (1969), sapphirine has been recognized as a chain silicate with the simplified crystallographic formula $M_8T_6O_{20}$, where M and T represent octahedral and tetrahedral sites, respectively. In MAS, octahedral positions in sapphirine are occupied by Mg and Al, while tetrahedral positions belong to Al and Si, and substitutions occur along the join Mg + Si = Al + Al, as implied by Higgins *et al*. (1979). Following our previous publications (Podlesskii, 1995; Gerya *et al*., 1996, 2004a), we accepted end-members $Mg_4Al_8Si_2O_{20}$ (Spr^S) and $Mg_3Al_{10}SiO_{20}$ (Spr^A) to represent the sapphirine solid solution for thermodynamic modeling in MAS. These end-members have also been chosen for the latest version of the THERMOCALC database (Kelsey *et al*., 2004), with which we will compare our results (earlier, THERMOCALC used end-members $Mg_4Al_8Si_2O_{20}$ and $Mg_{3.5}Al_9Si_{1.5}O_{20}$). In terms of the Tschermak type substitution Mg + Si = Al + Al, a wider range of the sapphirine solid solution will probably be considered in future studies, since sapphirines with more than 2 Si per formula unit have been observed both in experiments (Milholland & Presnall, 1998; Liu & Presnall, 2000; Das *et al*., 2001, 2003; Liu & O'Neill, 2004), and in nature, namely cracks in pyrope megablasts from Dora-Maira, Italian Alps (Simon & Chopin, 2001), whereas sapphirine with less than 1 Si per formula unit has been encountered in eclogites from the South Carpathians, Romania (Sabau *et al*., 2002).

In our approach, sapphirine solid solution (Spr) was initially considered as an ideal mixture of end-members Spr^S and Spr^A (often referred to as "2:2:1" and "3:5:1", respectively, in the literature). Unlike Kelsey *et al*. (2004), we found that describing the existing experimental data did not require non-ideality. However, non-ideality can be introduced by analogy with other minerals that demonstrate the Tschermak substitution, and we have also tried the non-ideal model, although this approach has added parameters not constrained by measurements. A composition parameter X_{SS} that denotes the mole fraction of Spr^S ranging from 1 to 0 has been used to represent the activity relationships. A regular solution parameter W_{Spr} has been used for the non-ideal model to express the excess energy dependence on composition as $W_{Spr} \cdot X_{SS} (1 - X_{SS})$.

Our experience (Podlesskii, 1995) shows that variation in sapphirine composition plays a decisive role for thermodynamic modeling of sapphirine-bearing equilibria, and it is impossible to describe the whole spectrum of existing experimental data with a constant composition, as was tried by Gottschalk (1997) with sapphirine $Mg_9Al_{18}Si_3O_{40}$ ("7:9:3") or Jung *et al*. (2004) with an out-of-date formula $Mg_4Al_{10}Si_2O_{23}$ ("4:5:2") of Foster (1950) that is in conflict with the structure determinations (Moore, 1969; Higgins & Ribbe, 1979; Merlino, 1980; Barbier & Hyde, 1988).

At present, effects of polytypism and stacking disorder on stability of sapphirine (Christy, 1989a and b) cannot be considered in terms of its thermodynamic properties due to the lack of data for the experiments under consideration, and this simplification undoubtedly introduces additional uncertainties.

Experimental data and their thermodynamic description

Experimental investigations related to MAS have a long history, since this system has become important for metallurgy and the ceramic industry (Jung *et al*., 2004 and the references therein) and petrology (Schreyer & Seifert, 1969a; Gasparik, 1994 and the references therein). However, experiments on melting and crystallization of various mixtures widely used in ceramic studies often did not provide evidence for achieving equilibrium relationships. They always involved phases of undefined composition, like melt, with the sapphirine composition having never been determined, although sometimes claimed to be close to 2:2:1 or 7:9:3. In the absence of fluid, reactions involving MAS phases are notoriously sluggish because the phases are so refractory, and thus often proceed *via* metastable intermediates; so with insufficient run durations, incompatible phase assemblages may be observed even when the temperatures are relatively high. For example, Shu *et al*. (2002) and Menchi & Scian (2005) reported the joint appearance of sapphirine and cristobalite at temperatures between 1200 °C and 1280 °C in crystallizing cordierite ceramics. Conversely, crystallizing a

mixture of cordierite + spinel with stoichiometry of sapphirine 2:2:1 at 900 °C and 1.5 GPa, Schreyer (1967) initially obtained orthopyroxene + corundum + spinel in a 22 h long run, and only in longer runs did the mixture yield 40 % of sapphirine. Forsterite was found in metastable coexistence with quartz in experiments at temperatures up to 1350 °C and pressures up to 2 GPa (Arima & Onuma, 1977).

To facilitate reactions in MAS and to get the run product grains large enough for electron microprobe analysis, Perkins *et al*. (1981) and Gasparik & Newton (1984) used fluxes, which yielded grains large enough to characterize solubility of alumina in orthopyroxene coexisting with pyrope or forsterite + spinel in detail and with confidence. This, in due course, resulted in a more reliable description of thermodynamic properties of orthopyroxene solid solution in MAS.

The only experimental determination of equilibrium sapphirine compositions is reported by Hollis & Harley (2003), which was not sufficient to get a confident description of the compositional variation with P and T (this issue will be addressed later in this paper). Most other authors either did not analyze product sapphirines or reported that the sapphirine grains were too small to be analyzed with the electron microprobe (*e.g.*, Chatterjee & Schreyer, 1972; Ackermand *et al*., 1975). Consequently, we used X_{SS} as one of the parameters that describes sapphirine-bearing reactions while fitting the experimental brackets. This was only possible for the reactions with minerals whose thermodynamic properties had already been well constrained by measurements and determination of sapphirine-free reactions. Equilibria with phases such as melt and mullite, which have variable and undetermined compositions, had to be excluded from the treatment. For the same reason, the reversals of sapphirine breakdown reactions involving chlorite in the system $MgO–Al_2O_3–SiO_2–H_2O$ (MASH) obtained by Seifert (1974) were also not treated, since equilibrium compositions of chlorite had not been determined in experiments and could not be constrained from thermodynamic data. The only MASH reversals treated were those of reaction orthopyroxene + sapphirine = cordierite + spinel. It is noteworthy that with the addition of water, the stability fields of MAS sapphirine-bearing assemblages either shrink dramatically towards higher temperatures or disappear, because H_2O-containing phases become stable. This hampers the experimental investigations under moderate temperatures and elevated pressures, since fluid-absent crystalline mixtures either do not react or react unacceptably slowly under these conditions. Podlesskii (1996) tried to circumvent this problem by adding anhydrous $MgCl_2$ to crystalline starting materials while investigating reaction orthopyroxene + spinel + corundum = sapphirine at 700–750 °C and 15–16 kbar. However, reaction was still slow, and sapphirine grains were still very small, so it was only possible to obtain preliminary constraints.

Thermodynamic properties of sapphirine end-members and other minerals have been estimated in terms of semi-empirical Equation (1) introduced by Gerya *et al*. (1996, 1998, 2004a and b) for expressing the Gibbs free energy (J/mol)

$$\begin{aligned} G_s = {} & H_{298.1} - T \cdot S_{298.1} + V^o_s \cdot \Psi + c_1 \cdot [RT \cdot \ln(1 - e_1) \\ & - \Delta H^o_{s1} \cdot (1 - T/T_0) \cdot e_{01}/(1 - e_{01}) \\ & - RT \cdot \ln(1 - e_{01})] + c_2 \cdot [RT \cdot \ln(1 - e_2) \\ & - \Delta H^o_{s2} \cdot (1 - T/T_0) \cdot e_{02}/(1 - e_{02}) \\ & - RT \cdot \ln(1 - e_{02})], \end{aligned} \quad (1)$$

where T is temperature (K); standard temperature T_0 = 298.15 K; P is pressure (bar); universal gas constant R = 8.313 (J/mol K); $e_i = \exp[-(\Delta H^o_{si} + \Delta V^o_s \cdot \Psi)/RT]$; $e_{0i} = \exp[-\Delta H^o_{si}/(R \cdot T_0)]$; $\Psi = 5 \cdot (1 + \phi)^{1/5} \cdot [(P + \phi)^{4/5} - (1 + \phi)^{4/5}]/4$ (bar); other parameters are shown in Table 1. In the case of non-ideal sapphirine, its end-member properties were obtained consistent with the integral and partial mixing energies

Table 1. Parameters of end-members for calculating the Gibbs free energy with Equation (1).

End-member	Formula	$-\Delta H_{298.1}$, J/mol	$S_{298.1}$, J/K mol	c_1	ΔH^o_{s1}, J	V^o_s, J/bar	ϕ, bar	$\Delta V^o_s \cdot 10^3$, J/bar	c_2	ΔH^o_{s2}, J
Qtz	SiO_2	910303	41.59	4.7513	3074	2.305	71406	4.0049	4.1759	10523
En	$MgSiO_3$	1545471	64.20	14.3025	5362	3.124	250489	4.6603	2.8493	24657
OK*	Al_2O_3	1672830	50.86	14.8854	5896	2.872	456483	3.0291	1.9663	27556
Crn	Al_2O_3	1673827	49.79	15.0305	5989	2.553	522202	3.5226	1.8833	30645
Fo	Mg_2SiO_4	2169792	95.14	20.0065	5144	4.350	250668	5.3655	4.2036	28433
Spl	$MgAl_2O_4$	2297275	84.91	20.8017	5575	3.967	404263	3.7376	3.6415	29111
Sil	Al_2SiO_5	2583627	95.96	22.3771	5641	4.980	231391	2.1234	4.0337	26131
Ky	Al_2SiO_5	2590904	83.54	23.3306	5992	4.406	241723	4.4135	3.6993	29794
And	Al_2SiO_5	2587717	91.34	22.9572	5838	5.139	258753	4.0850	2.9233	25055
Prp	$Mg_3Al_2Si_3O_{12}$	6281474	262.60	56.9093	5384	11.295	323482	3.5274	8.4103	24574
Crd	$Mg_2Al_4Si_5O_{18}$	9161186	403.14	80.4590	5496	23.302	160366	0.9514	16.2280	28331
Spr^S	$Mg_4Al_8Si_2O_{20}$	11018469	413.75	98.8224	5405	19.861	387809	3.3426	13.9675	22093
Spr^A	$Mg_3Al_{10}SiO_{20}$	11168243	379.67	98.0793	5383	19.667	460442	3.3064	16.6157	20434
Spr^S**	$Mg_4Al_8Si_2O_{20}$	11003035	425.32	98.0066	5405	19.861	387809	4.1798	16.9013	22093
Spr^A**	$Mg_3Al_{10}SiO_{20}$	11181724	367.94	96.2787	5146	19.651	460442	2.1747	14.0486	20434

*Fictive orthopyroxene end-member; **end-member properties for the non-ideal solid solution.

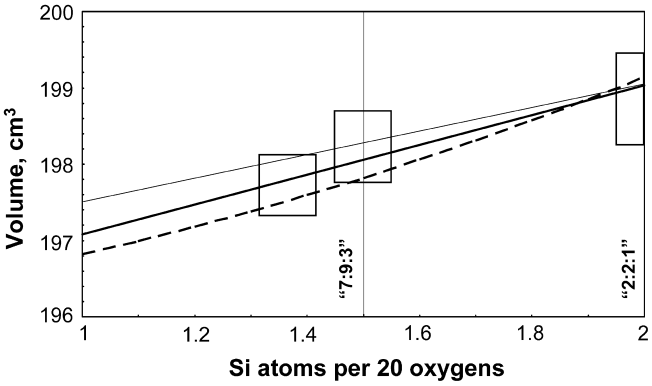

Fig. 1. The compositional dependence of sapphirine molar volume in MAS. Rectangles represent the measurements with uncertainties ±0.2 % for molar volume and ±0.05 for Si per 20 oxygens. Heavy line – our model for the ideal solution; dashed line – our model for the non-ideal solution; thin line – Kelsey *et al.* (2004).

$$G^m = RT \cdot [(1 - X_{SS}) \cdot \ln(1 - X_{SS}) + X_{SS} \cdot \ln(X_{SS})] + (1 - X_{SS}) \cdot X_{SS} \cdot W_{Spr} \quad (2)$$

$$G^m_{SprS} = RT \cdot \ln(X_{SS}) + (1 - X_{SS})^2 \cdot W_{Spr} \quad (2a)$$

$$G^m_{SprA} = RT \cdot \ln(1 - X_{SS}) + X^2_{SS} \cdot W_{Spr}, \quad (2b)$$

where $W_{Spr} = -4343 - 9.832 \cdot T - 0.06355\,(P - 1)$.

We have extracted the volume characteristics of sapphirine from measurements of unit cell parameters of synthetic sapphirines by Schreyer & Seifert (1969a), Seifert (1974), Newton *et al.* (1974), Bishop & Newton (1975), Charlu *et al.* (1975), Steffen *et al.* (1984) and Christy *et al.* (2002). As no analytical data have been provided by the authors for sapphirines 2:2:1 and 7:9:3, we believe that the crystallographic parameters correspond to the nominal compositions of starting mixtures within the uncertainty of ±0.05 Si per 20 oxygens. In case of the most aluminous sapphirine synthesized and analyzed by Bishop & Newton (1975), the composition was calculated to correspond to 1.367 Si per 20 oxygens. The unit cell volumes were calculated for the space group $P2_1/a$, which in some cases differed from those calculated for the space group $P2_1/n$ by authors of the measurements (*e.g.*, Schreyer & Seifert, 1969a). The derived V–X_{ss} dependence is shown in Fig. 1. In the case of non-ideal sapphirine, this dependence was described using a small negative volume of mixing parameter (see W_{Spr} above) consistent with the other thermodynamic properties, which were obtained by simultaneous treatment of all experimental data. Obviously, existing constraints on the V–X_{ss} dependence are relatively loose, which adds ambiguity to thermodynamic modeling.

Table 1 also presents an internally consistent set of parameters for other minerals relevant to MAS. They have been obtained by processing experimental data for the system CaO–FeO–MgO–Al_2O_3–SiO_2–K_2O–Na_2O by Gerya *et al.* (2004a). In the treatment of experimental data and calculations with this dataset, mixing properties of En and OK, respectively, the $MgSiO_3$ and Al_2O_3 end-members of orthopyroxene solid solution (Opx), were obtained as corresponding derivatives of the integral mixing energy

$$G^m = RT \cdot [(1 - 2 \cdot X_{OK}) \cdot \ln(1 - 2 \cdot X_{OK}) + 2 \cdot X_{OK} \cdot \ln(2 \cdot X_{OK})]/2 + (1 - 2 \cdot X_{OK}) \cdot X_{OK} \cdot [W_{MA} + W_{AM} \cdot (1 - 4 \cdot X_{OK})], \quad (3)$$

i.e.,

$$G^m_{OK} = G^m + (1 - X_{OK}) \cdot \partial G^m / \partial X_{OK}, \quad (3a)$$

$$G^m_{En} = G^m - X_{OK} \cdot \partial G^m / \partial X_{OK}, \quad (3b)$$

where X_{OK} is the mole fraction of OK, *i.e.*, the number of Al atoms per 3 oxygens; $W_{MA} = 53616.5 - 22.6953 \cdot T - 0.08454 \cdot (P - 1)$; $W_{AM} = -16170.5 + 3.6511 \cdot T - 0.03899 \cdot (P - 1)$. To account for the activity change of cordierite under water-saturated conditions, the model proposed by Aranovich & Podlesskii (1989) was used, *i.e.*, $G^w = -10099.4 + T \cdot 8.1833 - 1.55751 \cdot (P - 1)$ was added to G_s values obtained for Crd with Eq. (1). The Gibbs free energy for quartz was calculated using Eq. (1) with addition of energy relative to the ordered state (Gerya *et al.*, 1998, 2004b) defined as:

$$\begin{aligned} G_\alpha = {} & c_1 \cdot (RT \cdot \ln\{[1 - \exp(-\Delta H^o_{s1}/R/T)] \\ & /([1 - \exp(-\Delta H^o_{s1}/R/T)] \\ & + \exp([-\Delta H_{s\lambda} \cdot X^2_\alpha - \Delta V_{s\lambda} \cdot \Psi]/R/T) \\ & \times [\exp(-\Delta H^o_{s1}/R/T) \\ & - \exp([-\Delta H^o_{s1} - \Delta V^o_s \cdot \Psi]/R/T)])\}) \\ & + c_2 \cdot (RT \cdot \ln\{[1 - \exp(-\Delta H^o_{s2}/R/T)] \\ & /([1 - \exp(-\Delta H^o_{s2}/R/T)] \\ & + \exp([-\Delta H_{s\lambda} \cdot X^2_\alpha - \Delta V_{s\lambda} \cdot \Psi]/R/T) \\ & \times [\exp(-\Delta H^o_{s2}/R/T) \\ & - \exp([-\Delta H^o_{s2} - \Delta V^o_s \cdot \Psi]/R/T)])\}) \\ & + \{RT \cdot [X_\alpha \cdot \ln X_\alpha + (1 - X_\alpha) \cdot \ln(1 - X_\alpha)] \\ & + (H_{ord} + V_{ord} \cdot \Psi) \cdot X_\alpha \\ & + (W_H + W_v \cdot \Psi) \cdot X_\alpha \cdot (1 - X_\alpha)\}/(1 + 2 \cdot X_\alpha), \end{aligned} \quad (4)$$

where X_α denotes the mole fraction of ordered clusters in quartz at $G_\alpha = \min$; $\Delta H_{s\lambda} = 12594.6$ J/mol; $\Delta V_{s\lambda} = 0.21922$ J/bar/mol; $H_{ord} = -2622.8$ J/mol; $V_{ord} = -0.12889$ J/bar/mol; $W_H = 14236.2$ J/mol; $W_V = 0.637$ J/bar/mol. Other minerals were treated as end-member phases.

In comparison to modeling with a sufficient set of independent reactions, a "full-scale" equation of state allows more

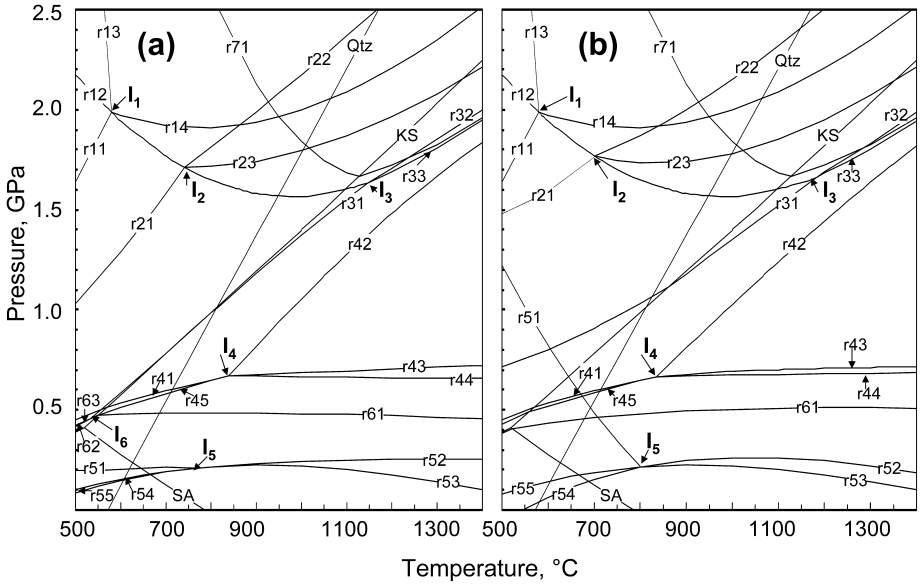

Fig. 2. P–T diagrams for the system $MgO–Al_2O_3–SiO_2$ calculated with data of Table 1 involving (a) ideal and (b) non-ideal solid solution models of sapphirine. Invariant points are marked as in the text. Reaction curves (high-pressure assemblage on the left-hand side): KS – Ky = Sil; SA – Sil = And; r11 – Fo + Crn = Opx + Spl; r12 – Prp = Opx + Crn; r13 – Prp + Spl = Fo + Crn; r14 – Prp + Fo = Opx + Spl; r21 – Opx + Spl + Crn = Spr; r22 – Prp + Spl + Crn = Spr; r23 – Prp + Spl = Opx + Spr; r31 – Opx + Crn =Spr + Sil(Ky); r32 – Prp + Crn = Opx + Sil; r33 – Prp = Opx + Spr + Sil; r41 – Opx + Sil(Ky) + Qtz = Crd; r42 – Opx + Sil = Spr + Qtz; r43 – Spr + Opx + Qtz = Crd; r44 – Spr + Qtz = Crd + Sil; r45 – Opx + Sil = Crd + Spr; r51 – Opx + Spl = Spr + Fo; r52 – Opx + Spr = Crd + Spl; r53 – Opx + Spl = Crd + Fo; r54 – Spr + Fo = Crd + Spl; r55 – Opx + Spr = Crd + Fo; r61 – Spr + Sil(Ky, And) = Crd + Crn; r62 – Opx + Crn = Crd + Spr; r63 – Opx + Ky = Crd + Crn; r71 – Prp + Qtz = Opx + Ky(Sil). Qtz – α–β Qtz transition. This numbering system is used throughout the text, tables and figures.

freedom for extrapolations. However, it also adds uncertainties related to additional parameters that are not constrained by direct determinations of individual thermodynamic properties and composition changes. Unfortunately, data on sapphirine itself are confined mostly to characterization of ordering phenomena, optical properties or spectroscopy (Burzo, 2004 and the references therein), which, at the moment, are of little help for describing the phase equilibria. Low- and high-temperature heat capacities were measured only for a natural sapphirine from Fiskenæsset that contained significant quantity of Fe^{2+} and Fe^{3+} and minor admixtures of Cr, Mn, Na and K (Nogteva *et al*., 1974; Kiseleva & Topor, 1975). Such an impure sapphirine is not suitable for calculating thermodynamic parameters. Measurements of low- and high-temperature heat capacities of synthetic sapphirines with well-determined compositions and determinations of their *P–V–T* behavior could make the estimates of EOS parameters less uncertain, and hopefully will be available in the future.

Petrogenetic grids calculated with thermodynamic data of Table 1 for both ideal and non-ideal sapphirine are shown in Fig. 2. Based on our internally consistent dataset of mineral properties, they have a topology similar in many important details to that calculated by Podlesskii (1995) with the set of internally consistent reaction properties. The grids involve two phases of variable composition, Opx and Spr, and seven phases of constant composition, Crd, Crn, Fo, Prp, Qtz, Sil (Ky, And) and Spl. Modeling with the ideal sapphirine produces six invariant points (named using absent-phase notation [ ]), I_1 – [Crd, Spr, Qtz, Sil (Ky, And)], I_2 – [Crd, Fo, Qtz, Sil (Ky, And)], I_3 – [Crd, Fo, Qtz, Spl], I_4 – [Fo, Prp, Crn, Spl], I_5 – [Crn, Prp, Qtz, Sil (Ky, And)] and I_6 – [Qtz, Fo, Prp, Spl], within a P–T range of 0.0001–2.5 GPa and 500–1400 °C. The non-ideal sapphirine model excludes I_6, because reactions Opx + Crn = Spr + Ky(Sil) (r31) and Spr + Sil = Crd + Sil (And) (r61) do not intersect since the reaction lines curve away from one another (Fig. 2), with sapphirine becoming more aluminous at lower temperatures. Reactions (r51) and (r21) involving non-ideal sapphirine must intersect at an invariant point [Crd, Prp, Qtz, Sil (Ky, And)] not far below 500 °C (actually estimated at 451 °C and 1.446 GPa), whereas with the ideal sapphirine, these two reactions probably intersect at temperatures too low to be accessible in Earth's crust.

Comparison of experimental data and calculated phase relations

Table 2 shows how our thermodynamic parameters describe experimental data on univariant reactions in MAS. Table 2 has been deposited and is freely accessible as supplementary material on the GSW website of the journal (http://eurjmin.geoscienceworld.org/). This description is also compared with calculations based on the data from Kelsey *et al*. (2004). Where high-pressure cells other than NaCl cells had been used in runs with piston-cylinder equipments, we applied friction corrections to the nominal pressures reported by the original authors. The corrections were made according to recommendations of Perkins *et al*. (1981) and Gasparik &

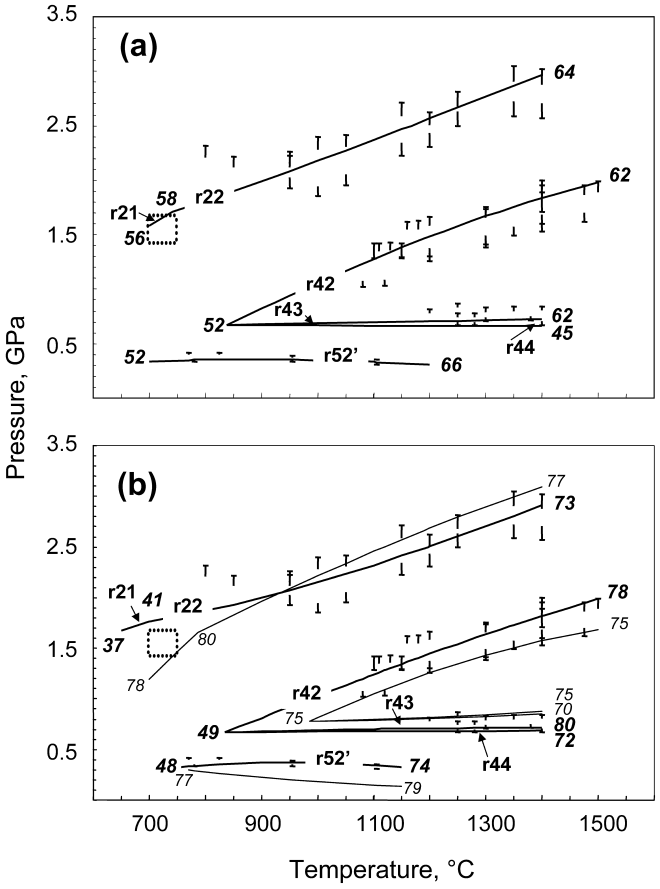

Fig. 3. Comparison of experimental data and calculations for reactions r21, r22, r42, r43, r44 and r52' (reaction r52 involving water-saturated cordierite) with (a) ideal and (b) non-ideal solid solution models of sapphirine. Experimental points represent brackets with the pressure values corrected for friction with 5 % error bars (see accepted values in text and in Table 2). Dotted area – preliminary experimental data for reaction r21 (Podlesskii, 1996). Heavy lines – our model; thin lines – Kelsey *et al*. (2004). Numbers show the calculated sapphirine composition ($N_{ss} = 100X_{ss}$) at ends of corresponding lines.

Newton (1984) for different types of cells. All pressure values were further adjusted by decreasing low-pressure limits and increasing high-pressure limits by 5 %, thus taking into account the uncertainties of the pressure measurements. Such an adjustment is reasonable (Gerya *et al*., 1998), bearing in mind that we did not correct the temperature values for uncertainties. The nominal, corrected and accepted values are shown in Table 2. Runs for which the original authors had reported "no reaction" were not considered, because there could be many reasons for the reactions not to proceed, and thus, the corresponding values may not refer to equilibrium conditions. Reaction brackets based on runs where directions of reactions had been observed proved to be sufficient for the analysis of phase relationships.

The two thermodynamic datasets demonstrate good agreement with sapphirine-free experiments, except that the description of reaction Opx + Spl = Crd + Fo with the THERMOCALC dataset is not quite satisfactory. Significant differences show up when sapphirine-bearing reactions are considered. As can be seen from Table 2 and Fig. 3, positions of the reactions calculated with our thermodynamic parameters agree with all the experimental brackets, whereas those calculated by Kelsey *et al*. (2004) are inconsistent with the experimental data of Seifert (1974) for the reaction Opx + Spr = Crd + Spl. The reactions calculated by Kelsey *et al*. (2004) also miss almost all brackets reported by Newton (1972) and Perkins *et al*. (1981) for Spr + Qtz (+Opx) = Crd, including that obtained at 1250–1280 °C and 7.2 ± 0.2 kbar in a gas apparatus, as well as brackets for Opx + Sil = Spr + Qtz at 1080, 1150 and 1200 °C by Chatterjee & Schreyer (1972), at 1100–1150 °C by Arima & Onuma (1977), at 1200 and 1400 °C by Newton (1972), and at 1400 °C by Hensen (1972). As a result, the Spr + Qtz stability field calculated with the THERMOCALC dataset is smaller than the field calculated from our dataset, and I_4 is shifted towards higher temperatures (986 °C *vs.* our 839 °C for ideal sapphirine and 835 °C for non-ideal sapphirine, Fig. 4).

Although, differing in calculated equilibrium compositions of sapphirine, our datasets and the dataset of Kelsey *et al*. (2004) produced coincident orthopyroxene compositions, which implies that the thermodynamic parameters of orthopyroxene must have been well constrained by sapphirine-free experiments, *i.e.*, the Al solubility in Opx associated with Prp, Spl + Fo or Crd + Qtz (Danckwerth & Newton, 1978; Perkins *et al*., 1981; Gasparik & Newton, 1984; Aranovich & Kosyakova, 1987) based on compositional brackets and electron microprobe analyses of Opx. In contrast, compositions calculated for the Opx + Spr + Qtz assemblage (Table 3) do not agree with the experimental data reported by Hollis & Harley (2003). The calculated Al contents of Opx differ from those experimentally determined both in values and in trends of their changes with *T* and *P*. Compared to the experimental determinations, the calculations give N_{OK} (a) a more gentle increase with increasing temperature at 1.2 GPa and (b) an increase with increasing pressure at 1325 °C (where $N_{OK} = 100X_{OK}$). This result implies negative slopes of the N_{OK} isopleths, *i.e.*, slopes opposite to those reported by Hollis & Harley (2003). Figure 4 illustrates the discrepancy between the calculated and the experimental compositions. The discrepancy is not related to the sapphirine solution model and originates from an irresolvable contradiction between the data by Hollis & Harley (2003) and calculated isopleths for Opx + Sil + Qtz and Opx + Crd + Qtz, which are tightly constrained by the above-mentioned data for Opx + Prp, Opx + Fo + Spl and Opx + Crd + Qtz. Having located reaction curves (r42) and (r43) directly from experimental data shown in Fig. 3 and using the data in Berman & Aranovich (1996), we have estimated the isopleths for Opx + Spr + Qtz (Fig. 4c), which also are contradictory to Hollis & Harley (2003) experiments. Unfortunately, there is no other source of measured compositions for Opx coexisting with Spr + Qtz to serve as a basis for comparison.

We can only assume that experiments by Hollis & Harley (2003) did not attain equilibrium with regard to compositions of orthopyroxene and sapphirine. These authors

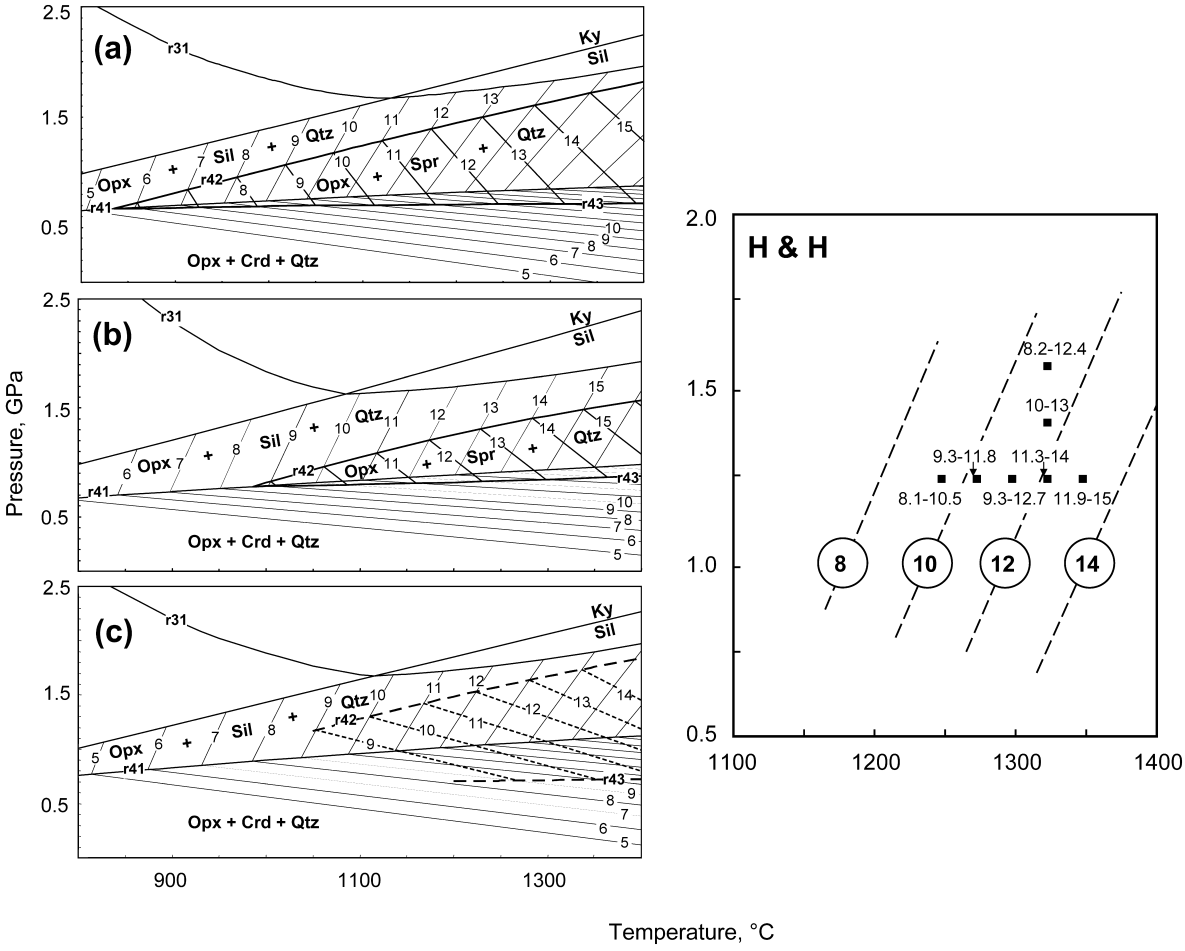

Fig. 4. Isopleths of the alumina content in Opx for assemblages Opx + Sil + Qtz, Opx + Crd + Qtz and Opx + Spr + Qtz in the system $MgO–Al_2O_3–SiO_2$. (a) Calculated with data of Table 1 (non-ideal solid solution of sapphirine); (b) calculated with the data from Kelsey *et al*. (2004); (c) calculated with data from Berman & Aranovich (1996) for assemblages Opx + Sil + Qtz and Opx + Crd + Qtz, and estimated for Opx + Spr + Qtz. Heavy lines – reaction curves; thin lines – isopleths (numbers denote mol.% Al_2O_3); solid lines – calculated; dashed lines – estimated. H & H – isopleths for assemblage Opx + Spr + Qtz (dashed lines with encircled numbers) and experimental points (filled squares with numbers showing the ranges of determined alumina contents) from Hollis & Harley (2003).

reported that no significant compositional trend in sapphirine could be resolved from the experimental data due to sluggish kinetics of this mineral. This may give us a possible explanation for the discrepancy between the calculated and the experimental data. If sapphirine reacted incompletely, then full equilibration of Opx is also in doubt. It should be noted that heterogeneity of the run product compositions slightly increased with increasing temperature, which may indicate that sapphirine started to react more readily only at higher *T*. It is noteworthy that the highest temperature runs at 1.2 GPa by Hollis & Harley (2003) did produce the Opx compositions consistent with the calculations (see Table 3). To interpret experiments involving more than one phase of variable composition with confidence, it is desirable that all solid solutions give a consistent sense of reaction direction (Berman & Aranovich, 1996), which seems not to be the case here. Experimental reversals of alumina content of orthopyroxene in assemblage with sillimanite and quartz, which is potentially a good geothermometer (Aranovich & Podlesskii, 1989; Podlesskii, 2003), could probably illuminate this problem, but they are not available at present.

Using criteria based on the appearance of different phases, Arima & Onuma (1977) estimated experimental Al contents of Opx associated with Spr + Qtz. Their lower temperature data indicate significantly lower Al contents compared to those derived with our models. However, it is unlikely their lower temperature Al contents are equilibrium values, since run products below 1350 °C contained Fo + Qtz. The high-temperature data with no Fo + Qtz present in the run products agree with our calculations: experimentally estimated contents of 15–16 wt.% Al_2O_3 at 1400 °C, and 16–17 wt.% Al_2O_3 at 1450 °C correspond to 15.4 and 16.0 wt.% Al_2O_3, respectively, calculated with ideal Spr, and to 15.4 and 16.1 wt.% Al_2O_3, respectively, with non-ideal Spr.

Our calculations are in reasonable agreement with experiments by Anastasiou & Seifert (1972), who estimated 3–5 wt.% Al_2O_3 at 900 °C and 5–7 wt.% at 1000 °C for Opx associated with Spr + Crd from the angular position of two X-ray reflections in the powder diffraction patterns of run products. We obtained with both ideal and non-ideal Spr 5.4 ± 0.4 % (uncertainty is related to P–T measurement errors) and 6.8 ± 0.4 %, respectively.

Table 3. Experimental determinations of mineral compositions in assemblage Opx + Spr + Qtz by Hollis & Harley (2003) compared to calculations with internally consistent datasets.

T, °C	Orthopyroxene, N_{OK}					Sapphirine, N_{SS}				
	Experimental			Calculated		Experimental			Calculated	
	Low*	High*	Median	1**	2**	Low*	High*	Median	1**	2**
					1.2 GPa***					
1250	8.1–9.8	10.4–11.3	9.1–10.5	**12.6**		64.6–76.4	65.6–75.8	70.5	**61.3**	
				12.7	**12.8**				72.3	75.5
1275	9.3–10	11.4–11.8	10.3–11	**13.0**		59.3–66.3	61.2–73.8	61.2–63.6	61.5	
				13.1	**13.2**				73.4	**75.5**
1300	9.3–9.5	11.9–12.7	11–11.2	**13.3**		58.7–94.1	66.5–73.4	64.6–70.5	61.7	
				13.4	**13.5**				74.5	75.5
1325	11.3–11.4	13.1–14	12.5	13.7		57.7–80.3	66.5–78.9	64.6–69.5	61.8	
				13.7	13.9				75.5	75.4
1350	11.9–12.4	14.7–15	13.4–13.7	14.1		59.6–70.5	58.7–87.6	65.2–70.5	61.9	
				14.1	14.3				76.4	75.4
					1.4 GPa***					
1325	10–12.2	10.5–13	11–11.5	**14.0**		63–72.4	63.8–75.6	67.5–71.3	**61.7**	
				14.0	**14.3**				74.7	75.3
					1.6 GPa***					
1325	8.2–11.8	10.2–12.4	10.4–11.3	**14.2**		66.5–80.3	64.6–73.8	69.3–72	**61.6**	
				14.3	**14.7**				73.9	75.2

*Low starting lower-alumina orthopyroxene; high – starting higher-alumina orthopyroxene, the composition data were taken from Fig. 2 and 3 of Hollis & Harley (2003); **1 calculated with data of Table 1 (upper value – ideal sapphirine, lower value – non-ideal sapphirine); 2 – calculated with data from Kelsey *et al*. (2004). ***Calculated values for pressures with −10 % correction for friction. Calculated values shown bold fall outside of the experimentally determined ranges.

Petrogenetic grids and implications for metamorphic rocks

Possible application of derived grids to petrologic interpretation may be related to sapphirine assemblages with quartz, kyanite and forsterite.

As shown in Fig. 2 and 5, the Spr + Qtz field extends to temperatures below 850 °C, which is closer to the initial estimate by Newton (1972), who supposed the invariant point to be located below 800 °C under anhydrous conditions and whose experimental data together with that of Chatterjee & Schreyer (1972) form a basis of our knowledge on stability limits of this assemblage in MAS (see Table 2). The sequence of reactions that belongs to this invariant point predicted by Chatterjee & Schreyer (1972) from graphical analysis proves to be qualitatively valid, but the calculated relations differ from the prediction in important quantitative details. It can be seen in Fig. 5 that reactions Opx + Sil + Qtz = Crd (r41) and Opx + Sil = Spr + Crd (r45) lie very close to each other in pressure, as do reactions Spr + Opx + Qtz = Crd (r43) and Spr + Qtz = Crd + Sil (r44). This implies that the presence of quartz must have little influence on the stability of Opx + Sil, and an addition of orthopyroxene to Spr + Qtz changes the stability of this assemblage only slightly. Under water-saturated conditions, the Spr + Qtz stability field shrinks due to the enhanced stability of hydrous cordierite, with the calculated invariant point I_4 being shifted along the Opx + Sil = Spr + Qtz reaction curve from 835 °C, 0.667 GPa to 1066 °C, 1.17 GPa (with ideal sapphirine, from 839 °C, 0.669 GPa to 1046 °C, 1.16 GPa). This agrees with experiments and further considerations of Newton (1972, 1995) concerning the magnesian cordierite stability and H_2O activity in high-grade metamorphism. Figure 5 also shows the effect of stabilization of cordierite at $P = P_{CO_2}$ estimated with the model of Aranovich & Podlesskii (1989). However, if we consider experimental data on reaction (r42), which are available only for temperatures above 1050 °C (Table 2; Fig. 3), and not their present interpretation, we would have to entertain the possibility that reaction curves (r41) and (r42) do not intersect to form I_4. This situation could result from the unpredictable non-ideal behavior of sapphirine, whereby Spr + Qtz is stabilized relative to Opx + Sil, and reaction curve (r42) acquires a concavity analogous to curve (r22) in Fig. 3b. With other experimental data unavailable for MAS at lower temperatures, the preliminary data of Podlesskii (1996) for reaction Spr = Opx + Spl + Crn (r21) provide the only obstacle for such modeling. One could easily dismiss these data by assuming that equilibration must have not been achieved in experiments at 700–750 °C. If such a model were proposed, it could have dramatic consequences related to elimination of I_4, which is the starting point of FMAS reaction Spr + Qtz = Opx + Sil + Crd (Podlesskii, 1997; Kelsey *et al*., 2004).

Another issue which may be important for interpretation of petrogenetic conditions is the stability field of Spr + Ky. This has been calculated with our data to exist below 816 °C and 1.015 GPa with ideal sapphirine, and below 862 °C and 1.128 GPa with non-ideal sapphirine, where reaction curve (r31) intersects the sillimanite–kyanite transition curve (Fig. 6). According to our calculations, ideal sapphirine must become significantly more aluminous along

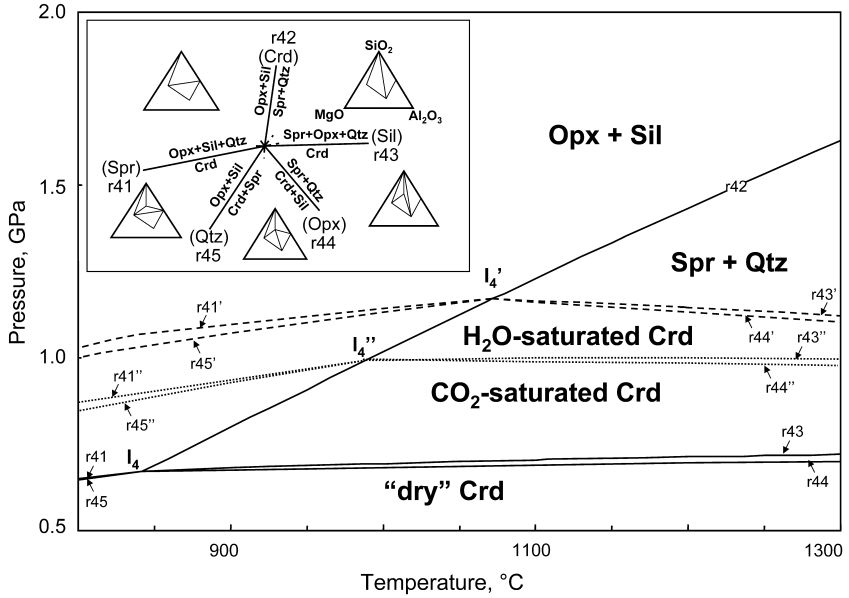

Fig. 5. Reactions belonging to invariant point I_4 calculated with the data of Table 1 (non-ideal sapphirine) for fluid-absent conditions (solid lines), $P = P_{H_2O}$(dashed lines) and $P = P_{CO_2}$(dotted lines) using the cordierite model proposed by Aranovich & Podlesskii (1989). Predictions from graphical analysis by Chatterjee & Schreyer (1972) are shown for comparison in the upper left corner.

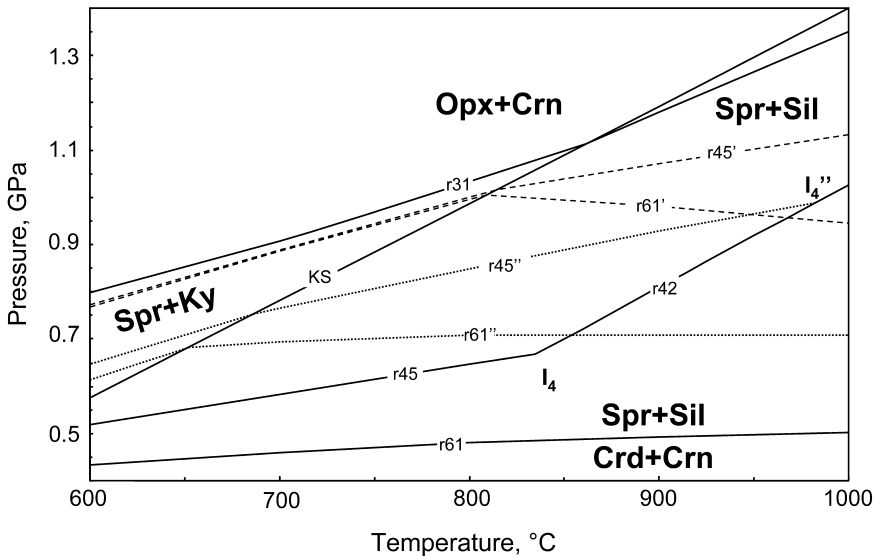

Fig. 6. The Spr + Ky stability field calculated with the data of Table 1 (non-ideal sapphirine) for fluid-absent conditions (solid lines), $P = P_{H_2O}$(dashed lines) and $P = P_{CO_2}$(dotted lines) using the cordierite model proposed by Aranovich & Podlesskii (1989).

(r31) starting with $N_{SS} = 60$ ($N_{SS} = 100X_{SS}$) at invariant point I_3 and ending with $N_{SS} = 33$ at I_6. Our estimates show that, with the non-ideal sapphirine solid solution, the Spr + Ky stability field is wider at lower temperatures, with N_{SS} changing from 49 at I_3 to 20 at 500 °C. Reactions involving the non-ideal sapphirine (r31) and (r61) do not intersect, either under fluid-absent condition, when reaction (r61) enters the And stability field at low temperatures, nor at $P = P_{H_2O}$ and $P = P_{CO_2}$ in the Ky stability field, because sapphirine becomes very alumina-rich and the reaction lines curve away from one another, thus excluding the existence of invariant point I_6. While investigating the stability field of gedrite in MASH, Fischer *et al.* (1999) observed the appearance of this phase together with Spr and Ky at 850 °C and 1.1 GPa, which can be considered as evidence supporting our non-ideal sapphirine model. In MASH, Spr + Ky must have a very limited stability field due to appearance of competing assemblages involving other hydrous phases, such as chlorite (Seifert, 1974) or boron-free kornerupine (Wegge & Schreyer, 1994).

The third remarkable assemblage (Spr + Fo) has been calculated to be stable at temperatures below invariant point I_5 (769 °C, 0.209 GPa with the ideal sapphirine model and 801 °C, 0.215 GPa – non-ideal; compare to 735 °C,

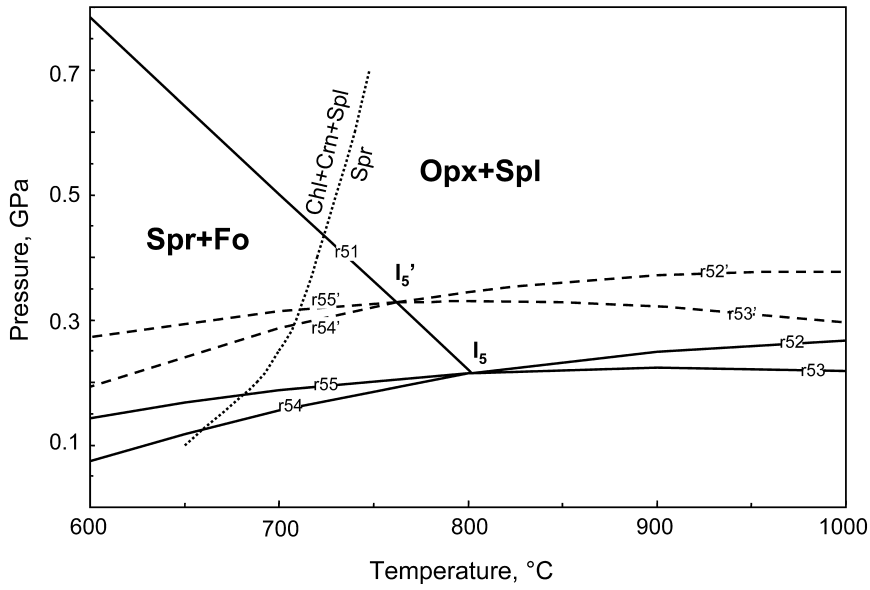

Fig. 7. The Spr + Fo stability field calculated with the data of Table 1 (non-ideal sapphirine) for fluid-absent conditions (solid lines) and $P = P_{H_2O}$(dashed lines) using the cordierite model proposed by Aranovich & Podlesskii (1989). The low-temperature stability limit of sapphirine at $P = P_{H_2O}$(dotted line) is shown according to experimental data of Seifert (1974).

0.209 GPa estimated by Podlesskii, 1995). Under water-saturated conditions, this assemblage does not appear in our calculations with the ideal sapphirine model at petrologically significant temperatures due to stabilization of cordierite, and the decrease of its stability calculated with the non-ideal model is shown in Fig. 7. In addition, hydrous phases like chlorite may also preclude the coexistence of sapphirine and forsterite in the wet system. Gasparik (1994) also obtained a narrow field of Spr + Fo at low temperatures, but we could not check its compatibility with experimental data on Opx + Spr = Crd + Spl and Opx + Spl = Crd + Fo, because the dataset presented by this author did not allow calculations with water-bearing cordierite.

Figure 8 presents our calculation of phase relations in MAS with the thermodynamic datasets of Holland & Powell (1998) and Kelsey *et al*. (2004). The former dataset, being a precursor of the latter, would not have been considered, if it had not been used by Ouzegane *et al*. (2003) as a basis for developing their own grid. As can be seen in Fig. 8, the data of Holland & Powell (1998) imply that Spr + Fo must preclude stability of competing assemblage Opx + Spl almost over the whole P–T space considered, which is in obvious conflict with much experimental and natural evidence of the wide P–T stability range of Opx + Spl. Grew *et al*. (1994), who predicted existence of invariant point I_5 at low temperatures under decreased water activity, emphasized a rarity of natural occurrences of Spr + Fo. The exaggerated stability of Spr + Fo implied by the THERMOCALC dataset might have been overlooked by Holland & Powell (1998) when they incorporated the sapphirine properties. The successor version presented by Kelsey *et al*. (2004) also implies an unrealistically wide stability field for Spr + Fo, although smaller than that of Holland & Powell (1998). Ouzegane *et al*. (2003), attempting "to derive pseudosections suitable for the studied rocks and the estimated P–T conditions" with the THERMOCALC data from Holland & Powell (1998), found that this could be achieved by adding −5 kJ/mol to the enthalpy of $Mg_2Al_8Si_2O_{20}$ and −10 kJ/mol to that of $Mg_{3.5}Al_9Si_{1.5}O_{20}$, thus increasing the stability of sapphirine. Obviously, this energy adjustment must cause even greater stability of Spr + Fo in relation to Opx + Spl, which has not been considered by the authors, who restricted themselves to consideration of certain granulites. Although their petrogenetic grid is undermined by the arbitrary adjustment comparable to univariant reaction energies, it should be noted that Ouzegane *et al*. (2003) must have considered the extended stability of Spr + Qtz in MAS (~ 850 °C, 0.7 GPa in their Fig. 12a) acceptable. In their interpretation of MAS, Spr + Ky must be stable at ~ 750–1100 °C and 0.8–1.7 GPa.

In other aspects, phase relations implied by successive versions of the THERMOCALC dataset look very similar to each other. As outlined above in relation to Spr + Qtz, the data presented by Kelsey *et al*. (2004) shift the stability field of this assemblage towards high temperature. This shift is likely due to inadequate fitting of thermodynamic properties to experimental data. At least in MAS, sapphirine can coexist with quartz at temperatures significantly below 900 °C.

Calculations with the THERMOCALC dataset, as can be seen in Fig. 8, do not allow sapphirine to coexist with kyanite in MAS. Evidently, this implies that stability of Spr + Ky must be even less possible in FMAS, because Fe preferably enters orthopyroxene, which must inevitably stabilize the competing Opx + Crn assemblage. Baldwin *et al*. (2007) tried to overcome the discrepancy between the observed presence of sapphirine + kyanite in nature and predictions by THERMOCALC just by excluding sillimanite from the list of phases involved in calculation of P–T relations, and interpreted their textures based on the Ca–FeO–MgO–Al_2O_3–SiO_2 grid, where "reactions dominantly

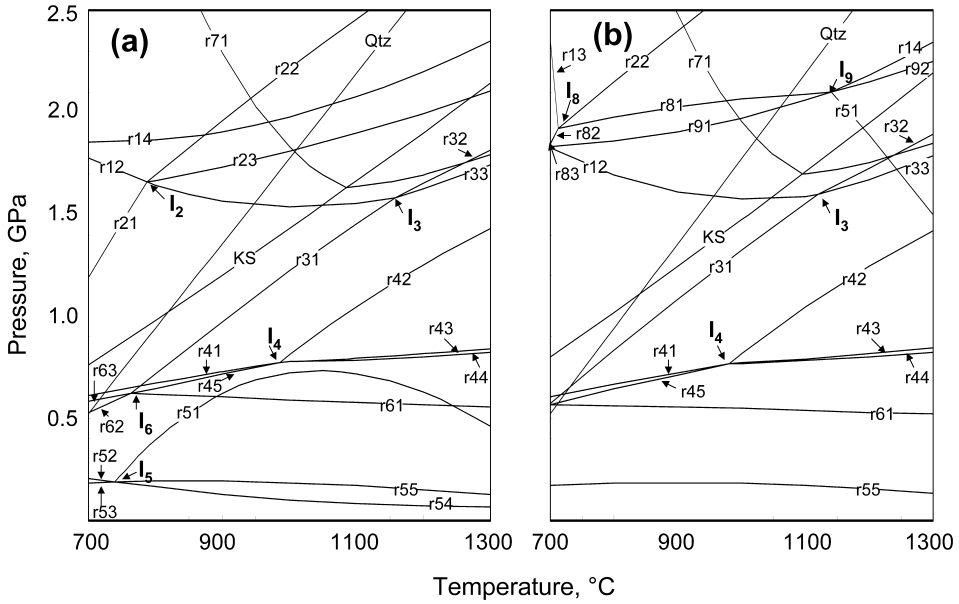

Fig. 8. P–T diagrams for the system $MgO–Al_2O_3–SiO_2$ calculated (a) with data from Kelsey *et al.* (2004) and (b) Holland & Powell (1998). Additional invariant points: I_8 – [Crd,Opx,Qtz,Sil(Ky,And)] and I_9 – [Crd,Crn,Qtz,Sil(Ky,And)]. Additional reaction curves: r81 – Prp + Spl = Spr + Fo; r82 – Fo + Crn = Prp + Spr; r83 – Fo + Spl + Crn = Spr; r91 – Prp + Fo = Spr + Opx; r92 – Prp + Spl = Spr + Opx.

lie within corundum + quartz stability" (their Fig. 10). Asami *et al.* (2007) described an FMAS sapphirine + spinel + kyanite + garnet ($X_{Mg} \approx 0.55$) assemblage meeting textural and chemical criteria of equilibrium in a granulite from the Sør Rondane Mountains, East Antarctica, but they were not successful in finding a stability field for this assemblage using THERMOCALC.

In our opinion, the outlined features of the THERMOCALC dataset simply reflect still insufficient knowledge of some major phase energetics, and in this regard, the statements of Powell & Holland (2008) that "pseudosections are likely to be the most effective form of thermobarometry for granulite facies and UHT rocks", and of Kelsey (2008) that "calculated phase diagrams allow the true complexity of mineral reaction topologies to be seen", appear to be somewhat premature. The example of sapphirine demonstrates that calculations of phase relations in complex chemical systems involving poorly constrained thermodynamic properties of minerals do not yet hold the advantage over "conventional" (the term introduced by Powell & Holland, 2008) thermobarometry based on either direct calibrations or thermodynamic datasets for experimentally well-constrained phases.

Concluding remarks

Critical assessment of phase equilibria involving sapphirine in MAS, as calculated using thermodynamic datasets, shows that there remain major inconsistencies between calculated and observed stability relationships. Better constraint is still needed for equilibria and thermodynamic properties, using reversal equilibration experiments and determination of equilibrium compositions of minerals. Optimized thermodynamic properties of the sapphirine solid solution imply that Spr + Qtz could be stable below 900 °C. Narrow stability fields of Spr + Ky are predicted at lower temperatures, and for Spr + Fo at very low water activity in accord with observed natural occurrences.

Although our description seems to fit most relevant experimental data, it should be noted that it is based on modeled compositions of sapphirine, and thus much uncertainty remains. One possible improvement to the sapphirine model would be an extension of the solid solution range beyond our limits of $2 > Si > 1$ per 20 oxygens, consistent with some natural sapphirines and Ge contents in Ga–Ge analogs reported by Barbier (1998).

Recently, Kelsey (2008) recognized that experimental data for systems other than MAS are not applicable to modeling of thermodynamic behavior of iron-bearing sapphirine, and switched to natural Fe–Mg partitioning data between sapphirine and coexisting orthopyroxene and garnet to get a bridge to FMAS and beyond. In this respect, he followed an approach earlier applied for the same purpose and reasons by Podlesskii (1995, 1997). However, the latter publications have demonstrated that even for FMAS, this method can produce alternative P–T diagrams with much lower temperatures of Spr + Qtz assemblages. They also had common features with the grid of Kelsey *et al.* (2004), such as the very close spacing of invariant points, which are to a great extent inherited from phase relationships defined by reactions belonging to the MAS invariant point I_4.

For modeling reactions involving sapphirine outside of MAS, it would be most desirable to obtain data that could define how other major constituents of this mineral, Fe^{2+} and Fe^{3+}, affect its properties. The thermodynamic

description of the effect of composition and P–T conditions on the stability of different polytypes of sapphirine could be another improvement. Since sapphirine in most cases has the highest Fe^{3+}/Fe^{total} ratio among coexisting Fe–Mg minerals, including aluminous spinel, these data could also shed light on redox conditions of metamorphism.

Acknowledgments: This work was inspired by Werner Schreyer at initial stages, when K.K.P. was an Alexander von Humboldt research fellow in Bochum. The authors are grateful to Simon Harley and Andrew Christy for their thorough and constructive reviews that stimulated us to improve the clarity of this paper. Our thanks are due also to Edward Grew for his extremely helpful comments and editorial assistance. The study was funded by RFBR grants 06-05-65069, 06-05-64976 and 06-05-64098-a.

References

Ackermand, D., Seifert, F., Schreyer, W. (1975): Instability of sapphirine at high pressures. *Contrib. Mineral. Petrol.*, **50**, 79-92.

Anastasiou, P. & Seifert, F. (1972): Solid solubility of Al_2O_3 in enstatite at high temperatures and 1–5 kb water pressure. *Contrib. Mineral. Petrol.*, **34**, 272-287.

Aranovich, L.Y. & Kosyakova, N.A. (1987): The cordierite = orthopyroxene + quartz equilibrium: laboratory data on and thermodynamics of ternary Fe–Mg–Al orthopyroxene solid solutions. *Geochemistry Int.*, **24**, 111-131.

Aranovich, L.Y. & Podlesskii, K.K. (1989): Geothermobarometry of high-grade metapelites: simultaneously operating reactions. *in* "Evolution of Metamorphic Belts", R.A. Cliff, B.W.D. Yardley, J.S. Daly, eds. *Geol. Soc. London Spec. Publ.*, **43**, 45-62.

Arima, M. & Onuma, K. (1977): The solubility of alumina in enstatite and the phase equilibria in the join $MgSiO_3$–$MgAl_2SiO_6$ at 10–25 kbar. *Contrib. Mineral. Petrol.*, **61**, 251-265.

Asami, M., Grew, E.S., Makimoto, H. (2007): Relict sapphirine + kyanite and spinel + kyanite associations in pyropic garnet from the eastern Sør Rondane Mountains, East Antarctica. *Lithos*, **93**, 107-125.

Baldwin, J.A., Powell, R., Williams, M.L., Goncalves, P. (2007): Formation of eclogite, and reaction during exhumation to mid-crustal levels, Snowbird tectonic zone, western Canadian Shield. *J. metamorphic Geol.*, **25**, 953-974.

Barbier, J. (1998): Crystal structures of sapphirine and surinamite analogues in the MgO–Ga_2O_3–GeO_2 system. *Eur. J. Mineral.*, **10**, 1283-1293.

Barbier, J. & Hyde, B.G. (1988): Structure of sapphirine: its relation to the spinel, clinopyroxene and β-gallia structures. *Acta Crystallogr.*, **B44**, 373-377.

Berman, R.G. & Aranovich, L.Y. (1996): Optimized standard state and solution properties of minerals. I. Model calibration for olivine, orthopyroxene, cordierite, garnet, and ilmenite in the system FeO–MgO–CaO–Al_2O_3–TiO_2–SiO_2. *Contrib. Mineral. Petrol.*, **126**, 1-24.

Bishop, F.C. & Newton, R.C. (1975): The composition of low pressure synthetic sapphirine. *J. Geol.*, **83**, 511-517.

Boyd, F.R. & England, J.L. (1959): Pyrope. *Carnegie Inst. Wash. Year Book*, **58**, 83-87.

Brigida, C., Poli, S., Valle, M. (2007): High-temperature phase relations and topological constraints in the quaternary system MgO–Al_2O_3–SiO_2–Cr_2O_3: an experimental study. *Am. Mineral.*, **92**, 735-747.

Burzo, E. (2004): Sapphirine and related silicates. *in* "Magnetic properties of non-metallic inorganic compounds based on transition elements: orthosilicates", H.P.J. Wijn, ed. *Landolt-Bornstein - Group III Condensed Matter, vol. 27, subvol. II (Orthosilicates)*, Springer-Verlag, 339-354.

Charlu, T.V., Newton, R.C., Kleppa, O.J. (1975): Enthalpies of formation at 970 K of compounds in the system MgO–Al_2O_3–SiO_2 from high temperature solution calorimetry. *Geochim. Cosmochim. Acta*, **39**, 1487-1497.

Chatterjee, N.D. & Schreyer, W. (1972): The reaction enstatite$_{ss}$ + sillimanite = sapphirine$_{ss}$ + quartz in the system MgO–Al_2O_3–SiO_2. *Contrib. Mineral. Petrol.*, **36**, 49-62.

Christy, A.G. (1989a): The effect of composition, temperature and pressure on the stability of the 1Tc and 2M polytypes of sapphirine. *Contrib. Mineral. Petrol.*, **103**, 203-215.

— (1989b): A short-range interaction model for polytypism and planar defect placement in sapphirine. *Phys. Chem. Minerals*, **16**, 343-351.

Christy, A.G. & Grew, E.S. (2004): Synthesis of beryllian sapphirine in the system MgO–BeO–Al_2O_3–SiO_2–H_2O and comparison with naturally occurring beryllian sapphirine and khmaralite, Part 2: a chemographic study of Be content as a function of *P*, *T*, assemblage and $FeMg_{-1}$ exchange. *Am. Mineral.*, **89**, 327-338.

Christy, A.G., Tabira, Y., Hölscher, A., Grew, E.S., Schreyer, W. (2002): Synthesis of beryllian sapphirine in the system MgO–BeO–Al_2O_3–SiO_2–H_2O and comparison with naturally occurring beryllian sapphirine and khmaralite. Part 1: experiments, TEM, and XRD. *Am. Mineral.*, **87**, 1104-1112.

Danckwerth, A. & Newton, R.C. (1978): Experimental determination of the spinel peridotite to garnet peridotite reaction in the system MgO–Al_2O_3–SiO_2 in the range 900–1100 °C and Al_2O_3 isopleths of enstatite in the spinel field. *Contrib. Mineral. Petrol.*, **66**, 189-201.

Das, K., Dasgupta, S., Miura, H. (2001): Stability of osumilite coexisting with spinel solid solution in metapelitic granulites at high oxygen fugacity. *Am. Mineral.*, **86**, 1423-1434.

—, —, — (2003): An experimentally constrained petrogenetic grid in the silica-saturated portion of the system KFMASH at high temperatures and pressures. *J. Petrol.*, **44**, 1055-1075.

Das, K., Fujino, K., Tomioka, N., Miura, H. (2006): Experimental data on Fe and Mg partitioning between coexisting sapphirine and spinel: an empirical geothermometer and its application. *Eur. J. Mineral.*, **18**, 49-58.

Doroshev, A.M. & Malinovsky, I.Yu. (1974): Upper pressure limit of stability of sapphirine. *Dokl. Akad. Nauk SSSR*, **219**, 136-138.

Fawcett, J.J. & Yoder Jr., H.S. (1966): Phase relations of the chlorites in the system MgO–Al_2O_3–SiO_2–H_2O. *Am. Mineral.*, **51**, 353-380.

Fischer, H., Schreyer, W., Maresch, W.V. (1999): Synthetic gedrite: a stable phase in the system MgO–Al_2O_3–SiO_2–H2O (MASH) at 800 °C and 10 kbar water pressure, and the influence of FeNaCa impurities. *Contrib. Mineral. Petrol.*, **136**, 184-191.

Foster, W.R. (1950): Synthetic sapphirine and its stability relations in the system MgO–Al_2O_3–SiO_2. *J. Am. Ceram. Soc.*, **33**, 73-84.

Friend, C.R.L. (1982): Al–Cr substitution in peraluminous sapphirines from Bjornesund area, Fiskenæsset region, southern West Greenland. *Mineral. Mag.*, **46**, 323-328.

Gasparik, T. (1994): A petrogenetic grid for the system MgO–Al_2O_3–SiO_2. *J. Geol.*, **102**, 97-109.

Gasparik, T. & Newton, R.C. (1984): The reversed alumina contents of orthopyroxene in equilibrium with spinel and forsterite in the system MgO–Al_2O_3–SiO_2. *Contrib. Mineral. Petrol.*, **85**, 186-196.

Gerya, T.V., Perchuk, L.L., Podlesskii, K.K., Kosyakova, N.A. (1996): Thermodynamic database for the system MgO–FeO–CaO–Al_2O_3–SiO_2. *Exp. Geosci.*, **5**, N2, 24-26.

Gerya, T.V., Podlesskii, K.K., Perchuk, L.L., Swamy, V., Kosyakova, N.A. (1998): Equation of state of minerals for thermodynamic databases used in petrology. *Petrology*, **6**, 511-526.

Gerya, T.V., Perchuk, L.L., Podlesskii, K.K. (2004a): Database and mineral thermobarometry program ''GEOPATH''. *in* "Experimental mineralogy: some results on the Century's Frontier", V.A. Zharikov & V.V. Fed'kin, eds. Nauka, Moscow, **2**, 188-206 (in Russian).

Gerya, T.V., Podlesskii, K.K., Perchuk, L.L., Maresch, W.V. (2004b): Semi-empirical Gibbs free energy formulations for minerals and fluids for use in thermodynamic databases of petrological interest. *Phys. Chem. Minerals*, **31**, 429-455.

Gottschalk, M. (1997): Internally consistent thermodynamic data for rock forming minerals in the system SiO_2–TiO_2–Al_2O_3–Fe_2O_3–CaO–MgO–FeO–K_2O–Na_2O–H_2O–CO_2. *Eur. J. Mineral.*, **9**, 175-223.

Grew, E.S., Chernosky, J.V., Werding, G., Abraham, K., Marquez, N., Hinthorne, J.R. (1990): Chemistry of kornerupine and associated minerals, a wet chemical, ion microprobe, and X-ray study emphasizing Li, Be, B and F contents. *J. Petrol.*, **31**, 1025-1070.

Grew, E.S., Yates, M.G., Romanenko, I.M., Christy, A.G., Swihart, G.H. (1992): Calcian, borian sapphirine from the serendibite deposit at Johnsburg, NY, USA. *Eur. J. Mineral.*, **4**, 475-485.

Grew, E.S., Pertsev, N.N., Yates, M.G., Christy, A.G., Marquez, N., Chernosky, J.V. (1994): Sapphirine + forsterite and sapphirine + humite group minerals in an ultra-magnesian lens from Kuhi-Lal, SW Pamirs, Tajikistan: are these assemblages forbidden? *J. Petrol.*, **35**, 1275-1293.

Grew, E.S., Yates, M.G., Shearer, C.K., Haggerty, J.J., Sheraton, J.W., Sandiford, M. (2006): Beryllium and other trace elements in paragneisses and anatectic veins of the ultrahigh-temperature Napier Complex, Enderby Land, East Antarctica: the role of sapphirine. *J. Petrol.*, **47**, 859-882.

Harley, S.L. (1998): On the occurence and characterization of ultrahigh-temperature crustal metamorphism. *in* "What Drives Metamorphism and Metamorphic Reactions?" P.J. Treloar & P.J. O'Brien, eds. *Geol. Soc. London Spec. Publ.*, **138**, 81-107.

— (2008): Refining the P–T records of UHT crustal metamorphism. *J. metamorphic Geol.*, **26**, 125-154.

Harley, S.L. & Christy, A.G. (1995): Titanium-bearing sapphirine in a partially melted aluminous granulite xenolith, Vestfold Hills, Antarctica: geological and mineralogical implications. *Eur. J. Mineral.*, **7**, 637-653.

Hensen, B.J. (1972): Phase relations involving $pyrope_{ss}$, $enstatite_{ss}$ and $sapphirine_{ss}$ in the system MgO–Al_2O_3–SiO_2. *Carnegie Inst. Wash., Year Book*, **71**, 421-427.

— (1986): Theoretical phase relations involving cordierite and garnet revisited: the influence of oxygen fugacity on the stability of sapphirine and spinel in the system Mg–Fe–Al–Si–O. *Contrib. Mineral. Petrol.*, **92**, 362-367.

Hensen, B.J. & Essene, E.J. (1971): Stability of pyrope–quartz in the system MgO–Al_2O_3–SiO_2. *Contrib. Mineral. Petrol.*, **30**, 72-83.

Hensen, B.J. & Green, D.H. (1971): Experimental study of the stability of cordierite and garnet in pelitic compositions at high pressures and temperatures: I. Compositions with excess alumino-silicate. *Contrib. Mineral. Petrol.*, **33**, 309-330.

Hensen, B.J. & Harley, S.L. (1990): Graphical analysis of P-T-X relations in granulite facies metapelites. *in* "High-temperature metamorphism and crustal anatexis", J.R. Ashworth & M. Brown, eds. Unwin Hyman, United Kingdom, 19–56.

Herzberg, C.T. (1983): The reaction forsterite + cordierite = aluminous orthopyroxene + spinel in the system MgO–Al_2O_3–SiO_2. *Contrib. Mineral. Petrol.*, **84**, 84-90.

Higgins, J.B. & Ribbe, P.H. (1979): Sapphirine. II. A neutron and X-ray diffraction study of $(Mg–Al)^{VI}$ and $(Si–Al)^{IV}$ ordering in monoclinic sapphirine. *Contrib. Mineral. Petrol.*, **68**, 357-368.

Higgins, J.B., Ribbe, P.H., Herd, R.K. (1979): Sapphirine. I. Crystal chemical contributions. *Contrib. Mineral. Petrol.*, **68**, 349-356.

Holland, T.J.B. & Powell, R. (1998): An internally-consistent thermodynamic dataset for phases of petrological interest. *J. metamorphic Geol.*, **16**, 309-343.

Hollis, J.A. & Harley, S.L. (2003): Alumina solubility in orthopyroxene coexisting with sapphirine and quartz. *Contrib. Mineral. Petrol.*, **144**, 473-483.

Jung, I.-H., Decterov, S. A., Pelton, A. D. (2004): Critical thermodynamic evaluation and optimization of the MgO–Al_2O_3, CaO–MgO–Al_2O_3 and MgO–Al_2O_3–SiO_2 systems. *J. Phase Equilib.*, **25**, 329-345.

Kelsey, D.E. (2008): On ultrahigh-temperature crustal metamorphism. *Gondwana Res.*, **13**, 1-29.

Kelsey, D.E., White, R.W., Holland, T.J.B., Powell, R. (2004): Calculated phase equilibria in K_2O–FeO–MgO–Al_2O_3–SiO_2–H_2O for sapphirine-quartz-bearing mineral assemblages. *J. metamorphic Geol.*, **22**, 559-578.

Kiseleva, I.A. & Topor, N.D. (1975): High-temperature heat-capacity of sapphirine (in Russian). *Geokhimiya*, **2**, 312-315.

Liu, T.-C. & Presnall, D.C. (2000): Liquidus phase relations in the system CaO–MgO–Al_2O_3–SiO_2 at 2.0 GPa: applications to basalt fractionation, eclogites, and igneous sapphirine. *J. Petrol.*, **41**, 3-20.

Liu, X. & O'Neill, H.St.C. (2004): Partial melting of spinel lherzolite in the system CaO–MgO–Al_2O_3–SiO_2 ± K_2O at 1.1 GPa. *J. Petrol.*, **45**, 1339-1368.

Malinovsky, I.Yu. & Doroshev, A.M. (1975): Low-pressure boundary of the stability field of pyrope: Experimental studies in mineralogy (in Russian), Akad. Nauk SSSR, Novosibirsk, 95-100.

Merlino, S. (1980): Crystal structure of sapphirine 1Tc. *Z. Kristallogr.*, **151**, 91-100.

Menchi, A.M. & Scian, A.N. (2005): Mechanism of cordierite formation obtained by the sol–gel technique. *Materials Lett.*, **59**, 2664-2667.

Milholland, C.S. & Presnall, D.C. (1998): Liquidus phase relations in the CaO–MgO–Al_2O_3–SiO_2 system at 3.0 GPa: the aluminous pyroxene thermal divide and high-pressure fractionation of picritic and komatiitic magmas. *J. Petrol.*, **39**, 3-27.

Moore, P.B. (1969): The crystal structure of sapphirine. *Am. Mineral.*, **54**, 31-49.

Newton, R.C. (1972): An experimental determination of the high-pressure stability limits of magnesian cordierite under wet and dry conditions. *J. Geol.*, **80**, 398-420.

— (1995): Simple-system mineral reactions and high-grade metamorphic fluids. *Eur. J. Mineral.*, **7**, 861-881.

Newton, R.C., Charlu, T.V., Kleppa, O.J. (1974): A calorimetric investigation of the stability of anhydrous magnesian cordierite with application to granulite facies metamorphism. *Contrib. Mineral. Petrol.*, **44**, 295-311.

Nogteva, V.V., Kolesnik, Y.N., Paukov, I.E. (1974): Low-temperature heat-capacity and thermodynamic properties of sapphirine (in Russian). *Geokhimiya*, **6**, 820-829.

Ouzegane, K., Guiraud, M., Kienast, J.R. (2003): Prograde and retrograde evolution in high-temperature corundum granulites (FMAS and KFMASH systems) from the In Ouzzal terrane (NW Hoggar, Algeria). *J. Petrol.*, **44**, 517-545.

Perkins III, D. (1983): The stability of Mg-rich garnet in the system CaO–MgO–Al_2O_3–SiO_2 at 1000–1300 °C and high pressure. *Am. Mineral.*, **68**, 355-364.

Perkins III, D., Holland, T.J.B., Newton, R.C. (1981): The Al_2O_3 contents of enstatite in equilibrium with garnet in the system MgO–Al_2O_3–SiO_2 at 15–40 kbar and 900–1600 °C. *Contrib. Mineral. Petrol.*, **78**, 99-109.

Podlesskii, K.K. (1995): Stability relations involving sapphirine in the system FeO–MgO–Al_2O_3–SiO_2. *Bochumer Geol. Geotech. Arb.*, **44**, 146-151.

— (1996): Sapphirine-bearing equilibria in the system MgO–Al_2O_3–SiO_2. *Terra Abstracts*, **8**, Suppl. 1, 51.

— (1997): P–T–X_{Mg} relations in aluminous granulites. *Exp. Geosci.*, **6**, 1, 22-23.

— (2003): Hypersthene in assemblage with sillimanite and quartz as an indicator of metamorphic conditions. *Trans. (Doklady) Rus. Acad. Sci./Earth Sci. Sec.*, **389**, 248-251.

Powell, R. & Holland, T.J.B. (2008): On thermobarometry. *J. metamorphic Geol.*, **26**, 155-179.

Sabau, G., Alberico, A., Negulescu, E. (2002): Peraluminous sapphirine in retrogressed kyanite-bearing eclogites from the South Carpathians: status and implications. *Int. Geol. Rev.*, **44**, 859-876.

Sato, K., Miyamoto, T., Kawasaki, T. (2006): Experimental calibration of sapphirine–spinel Fe^{2+}–Mg exchange thermometer: implication for constraints on P–T condition of Howard Hills, Napier Complex, East Antarctica. *Gondwana Res.*, **9**, 398-408.

Schreyer, W. (1967): A reconnaissance study of the system MgO–Al_2O_3–SiO_2–H_2O at pressures between 10 and 25 kbar. *Carnegie Inst. Wash., Year Book*, **66**, 380-392.

— (1968): Stability of sapphirine. *Carnegie Inst. Wash., Year Book*, **67**, 389-392.

Schreyer, W. & Abraham, K. (1975): Peraluminous sapphirine as a metastable reaction product in kyanite-gedrite talc shist from Sar e Sang, Afghanistan. *Mineral. Mag.*, **40**, 171-180.

Schreyer, W. & Schairer, J.F. (1961a): Stable and metastable phase relations in the system MgO–Al_2O_3–SiO_2. *Carnegie Inst. Wash., Year Book*, **60**, 144-147.

—, — (1961b): Compositions and structural states of anhydrous Mg-cordierites: a re-investigation of the central part of the system MgO–Al_2O_3–SiO_2. *J. Petrol.*, **2**, 324-406.

Schreyer, W. & Seifert, F. (1969a): High-pressure phases in the system MgO–Al_2O_3–SiO_2–H_2O. *Am. J. Sci.*, **267A**, Schairer volume, 407–443.

—, — (1969b): Compatibility relations of the aluminium silicates in the system MgO–Al_2O_3–SiO_2–H_2O and K_2O–MgO–Al_2O_3–SiO_2–H_2O at high pressures. *Am. J. Sci.*, **267**, 371-388.

—, — (1970): Pressure dependence of crystal structures in the system MgO–Al_2O_3–SiO_2–H_2O at pressures up to 30 kb. *Phys. Earth Planet. Interiors*, **3**, 422-430.

Schreyer, W. & Yoder, H.S. (1960): Instability of anhydrous Mg-cordierite at high pressure. *Carnegie Inst. Wash., Year Book*, **59**, 90-91.

Schreyer, W., Abraham, K., Behr, H.J. (1975): Sapphirine and associated minerals from the kornerupine rock of Waldheim Saxony. *N. Jb. Mineral. Abh.*, **126**, 1-27.

Schreyer, W., Horrocks, P.C., Abraham, K. (1984): High-magnesium staurolite in a sapphirine-garnet rock from the Limpopo belt, South Africa. *Contrib. Mineral. Petrol.*, **86**, 200-207.

Seifert, F. (1974): Stability of sapphirine: a study of aluminous part of the system MgO–Al_2O_3–SiO_2–H_2O. *J. Geol.*, **82**, 173-204.

Sheng, Y.J., Hutcheon, I.D., Wasserburg, G.J. (1991): Origin of plagioclase-olivine inclusions in carbonaceous chondrites. *Geochim. Cosmochim. Acta*, **55**, 581-599.

Shu, C., Mingxia, X., Cailou, Z., Jiaqi, T. (2002): Fabrication of cordierite powder from magnesium-aluminum hydroxide and sodium silicate: its characteristics and sintering. *Materials Res. Bull.*, **37**, 1333-1340.

Simon, G. & Chopin, C. (2001): Enstatite-sapphirine crack-related assemblages in ultrahigh-pressure pyrope megablasts, Dora-Maira massif, western Alps. *Contrib. Mineral. Petrol.*, **140**, 422-440.

Steffen, G., Seifert, F., Amthauer, G. (1984): Ferric iron in sapphirine: a Mössbauer spectroscopic study. *Am. Mineral.*, **69**, 339-348.

Wegge, S. & Schreyer, W. (1994): Boron-free kornerupine: its upper pressure stability limit in the system MgO–Al_2O_3–SiO_2–H_2O (MASH). *Eur. J. Mineral.*, **6**, 67-75.

Received 19 March 2008
Modified version received 17 June 2008
Accepted 7 July 2008